Polymer 68 (2015) 47–56

Contents lists available at ScienceDirect

Polymer

journal homepage: www.elsevier.com/locate/polymer

Influence of C_{60} fullerenes on the glass formation of polystyrene

Alejandro Sanz [a, 1], Him Cheng Wong [a, 2], Alisyn J. Nedoma [a], Jack F. Douglas [b], João T. Cabral [a, *]

[a] Department of Chemical Engineering, Imperial College London, London SW7 2AZ, UK
[b] Materials Science and Engineering Division, National Institute of Standards and Technology, Gaithersburg, MD 20899, USA

ARTICLE INFO

Article history:
Received 3 February 2015
Received in revised form
28 April 2015
Accepted 1 May 2015
Available online 12 May 2015

Keywords:
Fullerenes
Polystyrene
Nanocomposites

ABSTRACT

We investigate the impact of fullerene C_{60} on the thermal properties and glass formation of polystyrene (PS) by differential scanning calorimetry (DSC) and dielectric spectroscopy (DS), for C_{60} concentrations up to 30% mass fraction. The miscibility and dispersibility thresholds of PS/C_{60} nanocomposites are first estimated by a combination of microscopy, small angle neutron scattering (SANS) and wide-angle X-ray scattering (WAXS) experiments, and these thresholds were found to be $\simeq$1 mass% and $\simeq$4 mass% C_{60}, respectively. The addition of C_{60} increases the glass-transition temperature (T_g) of rapidly precipitated PS composites, up to a 'threshold' C_{60} concentration ($\simeq$4 wt%, in agreement with the dispersibility estimate). Beyond this concentration, the T_g reverts gradually towards the neat PS value. We present a comprehensive study for composites based on PS of molecular mass 270 kg/mol, and demonstrate the generality of the impact of C_{60} on T_g for PS matrices of 2 and 20 kg/mol. Thermal annealing or slowly evaporated composites largely reverse these effects, as the dispersion quality decreases. The dynamic fragility m of the composite is found to increase in the presence of C_{60}, but the scaling of m with T_g for PS is retained. Similarly, physical ageing experiments show a reduction of relaxation enthalpy in the glass regime, which is largely accounted for by the increase of T_g with C_{60}. The slowing down of the PS α-relaxation with C_{60} contrasts with the local 'softening' indicated by former Debye-Waller measurements and increase in fragility m. This effect is opposite to that of antiplasticizer additives, which both stiffen the material in the glassy state and reduce T_g, and simulations suggest this could be due to an increase in packing frustration. Finally, we review observations on the effect of nanoparticles on the T_g of PS and discuss the non-universal nature of T_g shifts by various types of nanoparticles.

1. Introduction

The introduction of nanoparticles to glass-forming polymers can lead to large property changes that are difficult to comprehend by extension of macroscopic filler effects and continuum theories of composite materials. Well-dispersed nanoparticles can dramatically enhance the stiffness (modulus, yield strength, toughness, scratch resistance), optical, thermal, electrical, fire-retardant and gas-transport properties [1–3]. These unique properties are usually rationalized in terms of the nanoparticle's inherently large surface-area-to-volume ratios and the comparable length scales between the particle size, inter-particle distance and radius of gyration R_g of macromolecules ($\approx$10 nm).

Nanoparticles have been shown to increase or decrease the glass transition temperatures T_g of polymers in a series of experiments [4–8] and empirical correlations involving polymer–particle interactions, particle–particle distances and total surface area have been suggested. Measurements and simulations [9] suggest that 'attractive' polymer–particle interaction may increase host polymer T_g, while nanoparticles with 'non-attractive' interactions tend to depress the T_g of polymers.

Analogies with polymer thin films are pertinent, as both are characterized by high interfacial areas and specific polymer–surface interactions [6]. In general, substantial reductions of T_g with decreasing film thickness L (when L becomes comparable to a monomer dependent packing length of the order of 100 nm) have been reported in both supported and free-standing films of polystyrene (PS) [10–12] and other relatively 'fragile' glass-forming

* Corresponding author.
E-mail address: j.cabral@imperial.ac.uk (J.T. Cabral).
[1] Present address: DNRF Center "Glass and Time", IMFUFA, NSM, Roskilde University, Universitetsvej 1, 4000 Roskilde, Denmark.
[2] Present address: Singapore University of Technology & Design, 8 Somapah Road, 487372, Singapore.

http://dx.doi.org/10.1016/j.polymer.2015.05.001

polymers [13]. However, supported polymer films on highly attractive surfaces often show positive T_g shifts when the thickness decreases, while the reverse has been observed for non-attractive substrates and free standing polymer thin films. Here too, the relief of packing frustration in thin films is expected to lower T_g, while the presence of attractive boundary interactions can increase segmental densities and increase T_g.

Given the nanoscale dynamic heterogeneity of glass-forming liquids, nanoparticles can be expected to influence such heterogeneity [9], and effectively the nature of the glass-formation process, including the strength of the temperature dependence rather than just the location of T_g. Understanding the impact of nanoparticles in polymer glass formation seems thus essential for the full exploitation of nanocomposites in practical applications.

The present work builds upon our previously published study by incoherent neutron scattering and calorimetry of PS/C_{60} composites [14,15]. We select this system as both the fullerene and polymer are well-defined, high purity, molecular species, and the 'nanoparticle' has an unambiguous surface chemistry and geometry. Further, fullerenes and derivatives find wide applications in thin film composites and organic photovoltaics [16,17].

We previously measured the effect of C_{60} on the high frequency dynamics of these polymer nanocomposite, and quantified how the addition of C_{60} altered the amplitude of atomic motions, estimated from the mean square amplitude $\langle u^2 \rangle$ femtosecond delocalizations expressed in the Debye-Waller factor, in the low temperature glassy state of the polymer nanocomposite [14]. We found that $\langle u^2 \rangle$ increases, albeit modestly, with the addition of C_{60} to PS ($\leq$ 1% mass fraction), indicating a reduction of the local 'stiffness' of the material in the glassy state. Recent molecular dynamics (MD) simulations [18] corroborate slower segmental dynamics and, interestingly, find a slight increase in dynamic heterogeneity of the composites. The authors report a restriction of local polymer motion, at variance with our neutron backscattering study [14] from (2–450) K (but in agreement with another study [19] which is, however, restricted to $T \geq 50$ K, known to be dominated by side-group motion [20]). Other studies [2] have indicated that the addition of nanoparticles to polymeric materials can increase the local free volume, as measured by positron annihilation measurements, along with corresponding increases in the permeability of the polymer material. Evidently, nanoparticles can disrupt the molecular packing of the neat polymer material, leading to more 'open' fluid structure at a nm scale or smaller. This is a finding with important ramifications.

We now consider explicitly the nanocomposite dispersion, and evaluate the impact of C_{60} on the glass formation of PS, in terms of T_g, physical ageing and dynamic fragility, measured by calorimetry and dielectric spectroscopy.

This paper is organised as follows. We first characterise dispersion by small angle neutron scattering (SANS), and wide angle X-ray scattering (WAXS), and evaluate fullerene cluster formation directly in polymer nanocomposite films by microscopy upon thermal annealing above T_g. We then systematically examine the variation of T_g with fullerene content as well as heat capacity change at the glass transition. Next we characterise the structural relaxation of the nanocomposite by dielectric spectroscopy which allows for the quantification of the nanocomposite fragility and independently estimate T_g from relaxation data. Once we characterised the quasi-equilibrium relaxation properties of the composite, we quantify the impact of dispersion upon thermal annealing and then the impact of physical ageing through specific heat measurements. We then discuss the combined implications of the present observations with our past neutron scattering measurements and finally we compare our res ults for PS-C_{60} to other PS nanocomposites where we seek an understanding of common trends.

2. Experimental

2.1. Nanocomposite preparation

A range of polystyrene-fullerene composites were prepared varying polymer molar M_W from 2.2 kg/mol to 270 kg/mol, fullerene C_{60} loading from 0 % to 30 % wt, and preparation method, namely by rapid precipitation (RP) and solution casting (SC). PS (BP Chemicals) was reprecipitated into a five-fold excess of methanol (99.5+%, GLC, Fisher Scientific) to remove impurities and characterized by Gel Permeation Chromatography (GPC) to have a molecular mass $M_W = 270$ kg/mol and polydispersity index $PDI = 2.3$. PS standards with $M_W = 2.2$ kg/mol, $PDI = 1.06$ (Pressure Chemicals), and $M_W = 22$ kg/mol, $PDI = 1.05$ (Polymer Source) were used as received [21]. C_{60} fullerenes (MER Corp., 99+% purity) were dissolved in a 0.2% mass fraction toluene solution (99.8+%, GLC, Fisher Scientific) and sonicated (CAMLAB Transsonic T570/H) for 30 min.

For the preparation of 'rapid precipitation' (RP) specimens [7], PS-C_{60}/toluene (10% mass fraction) solutions were sonicated for 30 min and stirred for 2 days at room temperature and finally precipitated in a 5-fold volume excess of methanol. Varying sonication conditions (0–150) min had no effect in thermal properties as measured by DSC for composites up to 2% C_{60}. Light purple fiber-composites are generally obtained upon precipitation, except for the highest C_{60} content solutions, which yield a yellow/brown powder. Samples were dried under vacuum (Binder VD23 with Edwards RV5 pump) at 100 °C, 10^{-2} mbar, for 3 days until no mass changes were detected.

'Solution cast' (SC) samples were prepared by casting from at (1–5) mass % solids mass fraction toluene solutions onto quartz and evaporating at ambient conditions, followed by vacuum drying as described above. Blends were prepared according to the measured solution phase behavior of PS/C_{60}/toluene reported previously [22,23], to avoid inadvertent fullerene precipitation induced by polymer addition.

Selected specimens were melt-pressed into films or micro-extruded. Hot pressing (2–30 min, 100–205 °C) into (100–200) μm films was carried out in a mould between Kapton sheets, gradually up 50 kN, and rapidly quenching to bellow T_g. A DSM micro-extruder TS/I-03 with recirculation was operated at 170 °C–180 °C, 150 rpm, for residence times of 10 min for extruded composites.

2.2. Microscopy

Blend morphology of spun cast films was probed by reflection optical microscopy (Olympus BX 41M), equipped with a CCD camera (AVT Marlin) and tapping-mode atomic force microscopy (Innova, Bruker AXS) using super sharp TESP-SS tips.

2.3. Small angle neutron scattering

Small-angle neutron scattering (SANS) measurements were carried out at time-of-flight diffractometer LOQ (ISIS, Oxfordshire) with a polychromatic $\lambda = 2$ Å–10 Å incident beam and fixed sample-to-detector distance of 4 m, covering a wavenumber window of $0.009 < q < 0.25$ Å^{-1}. Samples of PS-C_{60} were pressed into 14 mm disks of 1 mm thickness and mounted on a motorized sample rack for SANS measurements. In order to investigate the structural stability of the composites, identical samples were annealed for 12 h above T_g (130 °C–170 °C). Spectra were

acquired for approximately 20 min, corrected for sample transmission and background, and then radially averaged and calibrated to absolute intensity (cm^{-1}). The neutron scattering length densities of hydrogenous PS and C_{60} are, respectively, $\rho(PS) = 1.41 \times 10^{-6}$ Å^{-2} and $\rho(C_{60}) = 5.6 \times 10^{-6}$ Å^{-2}. Well dispersed composites are expected to scatter isotropically in this q range, while fractal (power law) scattering is expected for agglomerated specimens.

2.4. Wide angle X-ray scattering

Wide angle X-ray scattering (WAXS) measurements were carried out using a PANalytical XPert PRO diffractometer equipped with an X-Celerator detector and Cu anode source (K_α $\lambda = 1.54$ Å). Nanocomposite specimens in the fiber form were packed into a 2 cm diameter × 1 mm thick disk sample holder. Both fresh and thermally annealed composites, subject to various annealing temperatures and times, were studied to evaluate C_{60} agglomeration and ensuing crystallization.

2.5. Differential scanning calorimetry

Differential scanning calorimetry (DSC) experiments were carried out using a TA Instruments Q2000, nitrogen-cooled, Tzero^{TM}, autosampler system. DSC measurements were performed under helium environment and temperature and heat capacity were calibrated using a sapphire standard. Thermal history was eliminated by ramping from 30 °C to 160 °C at 10 °C/min, isothermal annealing at 160 °C for 1 min, then cooling at 40 °C/min−30 °C. The glass transition temperature T_g and heat capacity step ΔC_p were computed from a second heating run at 10 °C/min, following the onset/mid-point criterion (intersection between the glass and midpoint tangents). Error bars in T_g and ΔC_p are estimated by the maximum deviation of three independent measurements, typically ±1 °C and (0.001–0.02) J/g °C (discussed below).

To probe the effect of fullerenes on physical ageing, after removal of thermal history (as above), nanocomposites were annealed at various ageing temperatures T_a for ageing times τ_a, then cooled at 60 °C/min−30 °C, and finally measured at 10 °C/min. Physical ageing is manifested in calorimetry by the appearance of an enthalpy peak superimposed to the heat capacity step associated to the liquid to glass transition. The area underneath the excess structural relaxation peak is the relaxation enthalpy H and depends on the proximity to the glass transition ($\Delta T = T_a - T_g$) [24,25]. The change in relaxation enthalpy during physical ageing (ΔH) is computed by finding the integral difference between the aged and unaged thermograms.

2.6. Dielectric spectroscopy

Specimens for dielectric spectroscopy were melt pressed to 80 μm films, sputtered with gold, mounted between circular gold electrodes (2 cm diameter and 200 μm thickness) and measured using a Novocontrol broad-band dielectric system with integrated ALPHA interface. Dielectric loss measurements $\varepsilon'' = Im(\varepsilon^*)$, where ε^* is the complex dielectric permittivity, were performed over a broad frequency window, 0.1 $s^{-1} < f < 10^6$ s^{-1} in a temperature range of 223 K < T < 473 K. The temperature is controlled by a nitrogen jet (QUATRO from Novocontrol) with 0.1 K precision during frequency sweeps. Both fresh and (in-situ) annealed composites were investigated.

3. Results and discussion

3.1. Structure and dispersion of polystyrene-fullerene mixtures

The dispersion quality of PS-C_{60} nanocomposites was first investigated by optical microscopy, shown in Fig. 1, and AFM (data not shown). Spun cast films on silicon were found to be uniform and homogenous at concentrations up to 4 %–5 % mass C_{60}. Upon annealing at 180 °C (>T_g(PS)), fullerene cluster nucleation is observed within minutes for films of >1 mass% C_{60} [26]. At sufficiently high loadings (≥4–5 mass%), spinodal-like patterns emerge [27], due to the correlated nucleation of C_{60}, and yield well-defined undulating topographies whose wavelength (λ) and amplitude (δh) are controlled by the processing parameters [27,26]. By contrast, films <1–2 mass% C_{60} remain uniform (until eventual dewetting after ≃10 h, as expected for 270k M_W PS films on silicon).

SANS evaluated fullerene aggregation in bulk RP samples, at lengthscales <100 nm, benefitting from the strong scattering contrast between C_{60} and the hydrogenous polymer matrix. These results are shown in Fig. 1: excess low-q scattering is attributed to fullerene clusters and lines indicate a characteristic q^{-4} power law, corresponding to Porod scattering, arising from sharp interfaces. Upon annealing above T_g, the scattering intensity of PS-C_{60} 4% increases as agglomeration proceeds, while PS-C_{60} 1% scattering which remains unchanged upon annealing, indicating polymer-fullerene miscibility up to ≃1% C_{60}.

In order to elucidate the nature of the observed clusters and extend our measurements to molecular lengthscales, WAXS measured of various RP nanocomposites were carried out, shown in Fig. 2. A spectrum for pure, solid C_{60}, with characteristic crystalline fingerprint, is provided for reference. Prior to annealing, 'fresh' RP nanocomposites only display crystalline C_{60} peaks at concentrations ≥5%, indicating the presence of C_{60} crystalline clusters, in agreement with the results above. We refer to this concentration as a *dispersibility* limit [7,28,15], below which fullerenes remain largely dispersed in the matrix, *prior* to thermal annealing.

Upon annealing above T_g, WAXS from PS-1% C_{60} remains unchanged (Fig. 2b), while crystalline peaks grow within a few (2–5) min in PS-5% C_{60} annealed at 180 °C (Fig. 2c). Combined real and reciprocal space measurements indicate that 'dispersed' composites with up to 5% C_{60} are obtained by RP or spin coating, but thermally stable composites form only up to (1–2) mass % C_{60} in PS-270k. We next examine the impact of fullerenes, in various states of dispersion, on the glass formation of PS using a combination of DSC and DS experiments.

3.2. Glass transition of fresh and aggregated PS-fullerene nanocomposites

Fig. 3 compiles the DSC thermograms of fresh PS270k-C_{60} nanocomposite glasses, prepared by rapid precipitation, as a function of C_{60} loading. The estimated T_g (onset-midpoint method) is indicated with a vertical tick on the DSC traces and plotted in Fig. 4a. The data shows an unequivocal increase of the T_g with C_{60} content up to 4% mass fraction loading, beyond which a decrease toward the values of the neat PS is observed. The larger error bars of T_g for particle loadings 10%–30% are believed to be caused by composition heterogeneity in the sample, accompanied by large-scale agglomeration (visible by microscopy), and corresponding larger variability of results. The maximum increase of T_g observed is approximately 4 °C. Measurements of T_g for PS20k and PS2k corroborate the increase of T_g with C_{60}, shown in Fig. 4c) and d), but the magnitude of the T_g increase of PS2k exceeds 10 °C for fine ly precipitated RP specimens and is, however, minimal in aggregated drop cast samples (Fig. 4d). Given the similar behavior observed for

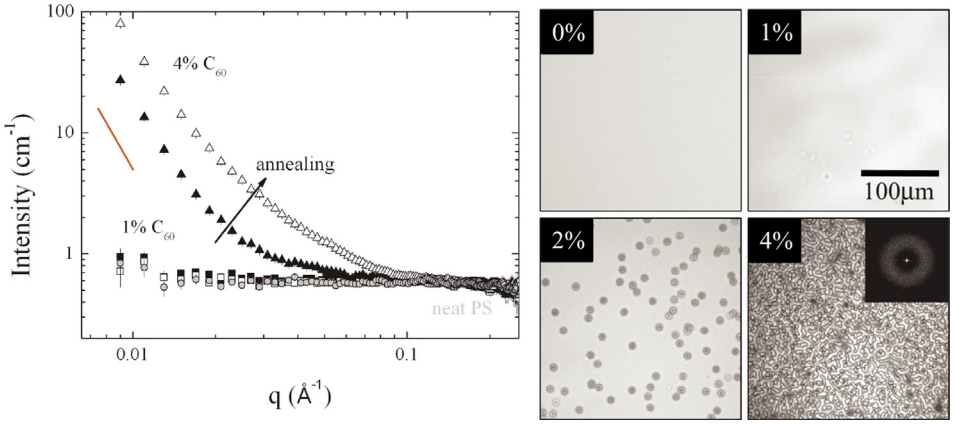

Fig. 1. Left: Small angle neutron scattering of PS270k-C_{60} bulk nanocomposites (■, □) 1% and (▲, △) 4% C_{60} by mass before and after annealing above T_g for 12 h (closed and open symbols respectively). The background (incoherent) scattering of hydrogenous polystyrene (○) is shown for comparison. Right: Optical micrographs of PS and PS-C_{60} thin films after annealing at 180 °C. The inset shows the FFT of the demixed morphology, which occurs between 1 and 2 wt% C_{60}.

the three M_W investigated in terms of the T_g dependence with fullerene content, we will focus henceforth on the PS270k-C_{60} series of samples.

Within the temperature range of these measurements, the heat capacity of neat C_{60} varies slowly [29,30], namely within (650–700) J/ °C mol or (0.90–0.97) J/ °C g over 90 °C–120 °C. At sufficiently low temperatures, a first-order transition from a simple cubic to face-centered-cubic structure, is expected at around −15 C in neat C_{60}, from DSC [29–31] and WAXS [31]. We can therefore rule out any non-trivial contribution of heat capacity of fullerenes in this range.

Above approximately 4%–5%, corresponding to the 'dispersibility' limit of our RP composites, the neat T_g of PS is slowly recovered. The increment in the heat capacity ΔC_p (half-width method) associated to the glass transition is represented as a function of the C_{60} content in Fig. 4b. For comparison purposes, ΔC_p has been normalized by the mass of the polymer matrix alone, but the behavior remains qualitatively unchanged if C_p (J/ °C) is normalized by total sample mass (PS–C_{60}). The ΔC_p is unchanged within experimental uncertainty up to 4% C_{60}, showing an measurable increase from 10% onwards. Molecular dynamics simulations of nanoparticles in polymer melts [32,33] have predicted a specific heat increase at the crossover between dispersed and clustered nanoparticle states, obtained from potential energy estimates of the particle configurations. We interpret this jump in ΔC_p as due to substantial clustering above 4 wt% C_{60} in the fresh composites.

Nanocomposite dispersion evidently affects the impact of any T_g shifts in the polymer matrix [7,34]. Fig. 5a and b shows the effect on the T_g of thermal annealing temperature and time for PS270k composites. The T_g of lower content C_{60} composites (<1%) remains unchanged for the temperature range investigated (up to 205 °C), at constant pressing time of 6 min. By contrast, the T_g of mixtures with higher C_{60} content 4% and 10% decreases with temperature, after ≈160 °C when diffusion is expected to be appreciable [35]. Annealing time does not appear to influence the T_g of PS270k-C_{60} 0.4%, as shown by the constancy of results obtained at 175 °C up to 30 min, and corroborated by SANS, WAXS and microscopy. Microextrusion was found to generally decrease T_g by approximately 1 °C–2 °C with respect to RP specimens, and GPC analysis reveals no chain scission takes place under our operating conditions. Solution cast films, shown to exhibit minimal T_g changes (Fig. 4d), exhibit clear C_{60} crystal transition endotherm around −15 °C (Fig. 5c), as expected for pure C_{60} [29–31] domains. The robustness of the experimentally determined T_g of PS-C_{60} nanocomposites to changes processing conditions corroborate the reproducibility of our experimental results and set requirements for 'nanocomposite' preparation.

Dielectric spectroscopy provides further insight into the influence of C_{60} fullerenes on the segmental dynamics of PS. Fig. 6 shows the dielectric loss measurements for (a) neat PS; (b) 1% and (c) 2%

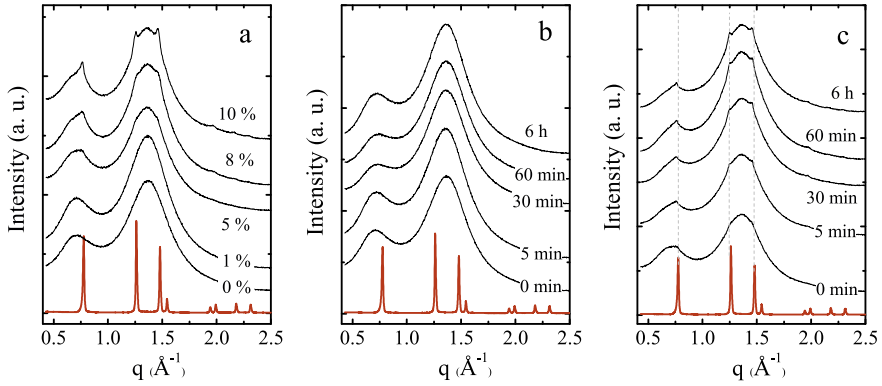

Fig. 2. (a) WAXS data of unannealed PS270k RP nanocomposites and (b) 1% C_{60} and (c) 5% C_{60} as a function of annealing time at 180 °C. The red data are the WAXS diffraction pattern of pure C_{60}. Crystalline C_{60} peaks (at $q = 0.77$, 1.26 and 1.48 Å^{-1}) appear in fresh composites with high ≥5% C_{60} loading and thermally annealed composites >≥1% C_{60}. Data scaled vertically for clarity. (For interpretation of the references to color in this figure legend, the reader is referred to the web version of this article.)

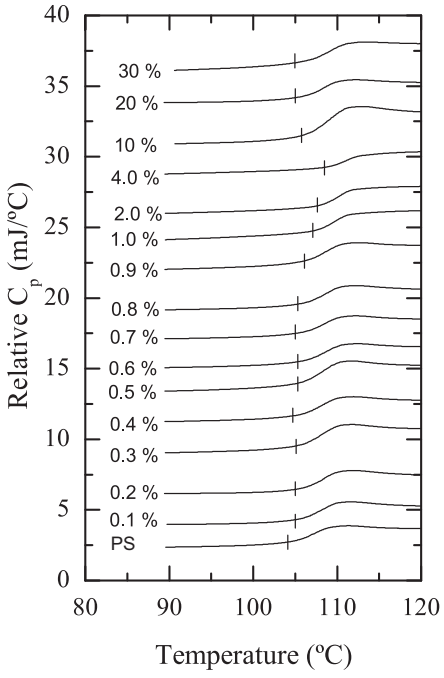

Fig. 3. DSC thermograms of fresh PS270k-C_{60} nanocomposites obtained at a temperature scanning rate of 10 °C/min, as a function of C_{60} content (0%–30% mass fraction). Vertical markers indicate the glass transition temperature T_g, defined by the onset/mid-point method (see text). Lines shifted for clarity.

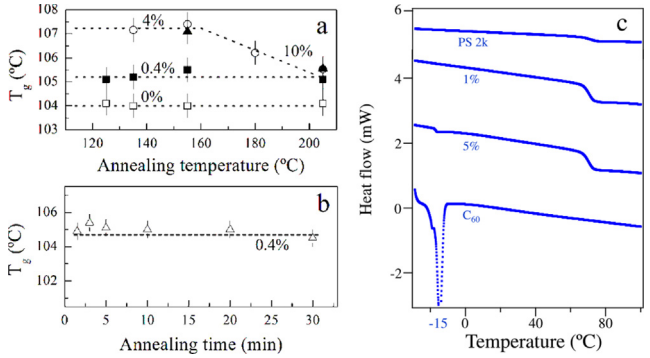

Fig. 5. (a) Glass transition temperature of T_g of PS270k composites with (■) 0.4%, (○) 4% and (▲) 10% C_{60} bulk films with melt press temperature (all 6 min) and (b) melt press time (175 °C). The lines serve as guide to the eye. (c) DSC thermograms of PS2k-C_{60} solvent cast composites showing, at sufficiently high concentration (≲5% C_{60}), the crystal transition of C_{60} at −15 °C visible in pure C_{60}.

C_{60}, respectively. PS has a rather low dipole moment and the β relaxation is thus not readily observed. Our analysis will, therefore, focus on the effect of C_{60} on the α relaxation of PS. The maximum observed in the dielectric loss data as a function of frequency corresponds to the α relaxation. In glass forming polymers, the α relaxation is a signature of the inter-chain correlation decay that takes place above T_g. The experimental dielectric relaxation curves were fitted to the empirical Havriliak-Negami equation (Eq. (1)), defined by a characteristic relaxation time τ_{HN}, angular frequency ω, the dielectric strength $\Delta\varepsilon$ and the broadening parameters b and c.

$$\varepsilon'' = \left(\frac{\sigma}{\varepsilon_0\omega}\right)^s + Im\left(\frac{\Delta\varepsilon}{\left[1+(i\omega\tau_{HN})^b\right]^c}\right) \quad (1)$$

The vertical lines indicate the location in frequency of the maximum peak for the neat PS relaxation curves, showing a shift towards lower frequencies of the α process in the presence of C_{60}. This slowing down of the PS segmental motions, most obvious in the low temperature range, agrees well with the increase of the T_g observed by calorimetric measurements.

In order to investigate the effect of the C_{60} aggregation on the dielectric response, in situ thermal annealing of the nanocomposites was carried out at 175 °C for 60 min. The effect of annealing on the α relaxation is shown in Fig. 7 for the PS270k-2% system, at selected measurement temperatures of 115 and 125 °C, prior and after annealing. The main observation is the displacement of the maximum loss to higher frequencies, recovering

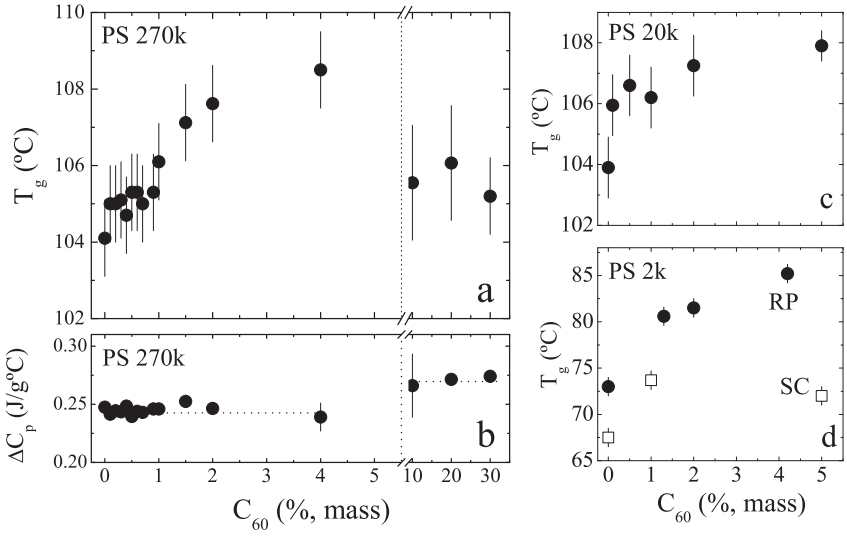

Fig. 4. Glass transition temperature of PS-C_{60} nanocomposites as a function of C_{60} concentration for (a) PS270k, (c) PS20k and (d) PS2k. The results generally show an increase in T_g with C_{60} for rapidly precipitated (RP) samples, which is (partly) reversed for drop cast samples, thermally annealed samples, or highly loaded composites. The magnitude of the T_g increase ranges from ≈4 °C (a,c) to 12 °C (d). Neat T_g values are gradually recovered beyond a mass fraction threshold of ≈4% C_{60}, shown for (a) PS270k, or (poorly dispersed) drop cast samples (d) PS2k. (b) Dependence of the heat capacity jump ΔC_p at the glass transition on the C_{60} mass fraction for PS270k-C_{60} composites. Dashed line indicates an apparent threshold associated with particle dispersibility in 'fresh' RP samples.

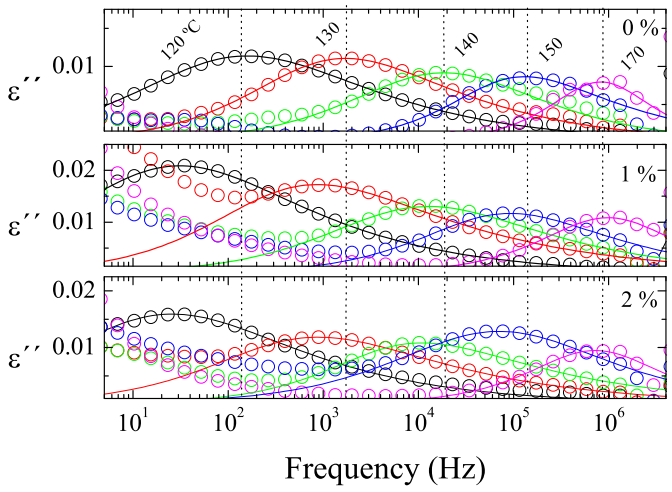

Fig. 6. Dielectric loss spectra of neat PS270k, PS-C_{60} 1% and 2% as a function of temperature showing the α relaxation.

approximately the characteristic values for neat PS sample. The dielectric curves at 115 °C and 125 °C for the PS matrix are included for comparison. The agglomeration of the C_{60} fullerenes obviously reduces the effective nanoparticle surface-to-volume ratio and therefore, reduces the restrictions to the PS chain segmental dynamics, making the PS-C_{60} dynamics essentially similar to neat PS.

Fig. 8a shows the evolution of the relaxation times, obtained from the maximum of the dielectric spectra (Fig. 6, as a function of the reciprocal temperature for PS270k and PS-C_{60} 1 and 2%. All samples show characteristic non-Arrhenius behavior, commonly observed for α relaxations, and the lines are best fits to the Vogel-Fulcher-Tamman (VFT) equation:

$$\tau_\alpha = \tau_0 \exp \frac{DT_0}{T - T_0} \tag{2}$$

where D is a strength parameter related to the dynamic fragility m through the following expresion: $m = 16 + 590/D$; T_0 is the Vogel temperature ($T_0 < T_g$) and τ_0 is a pre-exponential factor related to phonon-like time scales at the high temperature limit. In order to control the fitting procedure, values of T_0 were a priori estimated to be around $T_g - 50$ K and fixed, while D and τ_0 were adjustable parameters.

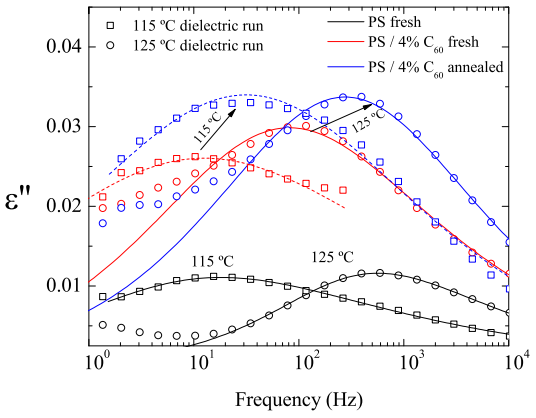

Fig. 7. Selected dielectric loss spectra obtained via isothermal frequency sweep ($T = 115$ °C (□) and 125 °C (○)) for PS270k (black) and PS-C_{60} 4% before (red) and after (blue) thermal annealing (175 °C, 60 min). (For interpretation of the references to color in this figure legend, the reader is referred to the web version of this article.)

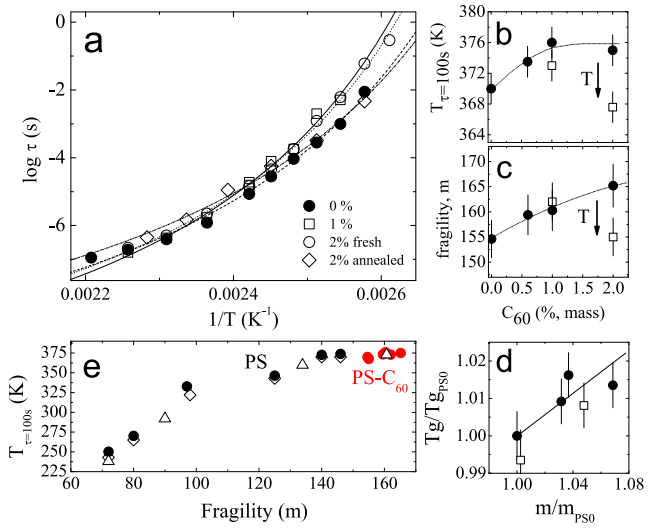

Fig. 8. (a) The relaxation map for neat PS270k (•), PS-1% C_{60} (□), PS-2% C_{60} (○) and annealed PS-2% C_{60} (◊)nanocomposites (175 °C, 60 min). The lines include best fit to the experimental data using Vogel-Fulcher-Tammann equation; (b) Dielectric T_g and (c) dynamic fragility as a function of C_{60} loading for 'fresh' (•) and annealed (□) (175 °C, 60 min) samples. Dielectric T_g is defined as the temperature at which $\tau_\alpha = 100$ s; (d) Correlation between T_g and fragility (m) of PS270k-C_{60} composites (normalized by neat PS values) 'fresh' (•) and annealed (□) specimens. (e) Compilation of T_g and m literature data for PS of various M_W ((△) [36], (•) [37], and ◊ [38]) and current PS270k composites (red •). (For interpretation of the references to color in this figure legend, the reader is referred to the web version of this article.)

This relaxation map indicates slower relaxation times for the fresh PS-C_{60} 1% and 2% composites in comparison to the neat PS, while the thermally annealed composites effectively revert back to pure PS response. The extrapolation of the VFT line to values of $\tau_\alpha = 100$ s gives the so called dielectric T_g (T_{g100s}) that is shown as function of C_{60} loading in Fig. 8b. As expected, T_{g100s} follows a similar trend to the calorimetric T_g, and the data also corroborate the return to neat PS behavior upon thermal annealing.

Further, a distinct temperature dependence is visible for both systems, which is quantified through the fragility index m, computed from the apparent activation energy around T_g, commonly used to classify glass forming materials [36–38]. Fig. 8c shows that m becomes larger with C_{60} content, indicating that fullerenes increase the dynamic fragility of PS. This finding is consistent with MD simulations [18] of this system. Upon thermal annealing, above the miscibility limit, these effects are again reversed as the fullerenes agglomerate. The relationship between T_g and m for our PS-C_{60} composites is plotted in Fig. 8d and found to be linear, within measurement uncertainty, as previously found in neat polymers [36] and predicted to hold for nanocomposites of various interactions [39].

For a given polymer matrix of varying M_W, well defined correlations between T_g and fragility m have been found experimentally, and are plotted for PS [36–38] in Fig. 8e. We find that our PS-C_{60} composites fall remarkable well with the correlation for neat PS, suggesting that the role of C_{60} is to simultaneously tune T_g and m of the polymer matrix, in an analogous fashion to changing M_W.

3.3. Physical ageing of polystyrene-fullerene mixtures

The influence of the C_{60} on the physical ageing of PS270k is further examined by calorimetry. A series of experiments probe the effect of ageing temperature $T_a < T_g$, ageing time τ_a and fullerene composition. The final heating scans are shown in Fig. 9 for neat PS and nanocomposites at 90 °C for τ_a up to 24 h. As expected, the

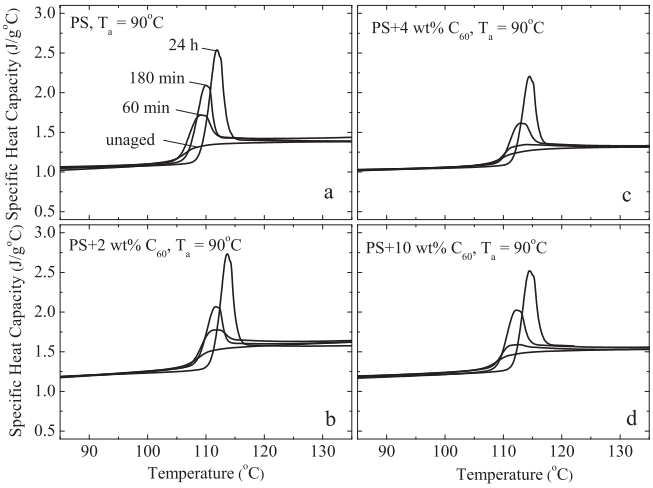

Fig. 9. DSC thermograms depicting the physical ageing of PS and PS-C_{60} nanocomposites at constant temperature (90 °C) for ageing times τ_a = (0, 60, 180, 1440) min.

relaxation enthalpy H increases with ageing time and depends on the proximity of ageing temperature to T_g where $\Delta T \equiv T_a - T_g$. ΔH ($H_{aged} - H_{unaged}$) at a given τ_a is expected to be small deep in the glassy state, goes through a maximum and then vanishes close to T_g. We find that the magnitude of relaxation enthalpy excess decreases with C_{60} content up to 4% (mass), with a slight reversal at 10% C_{60} additive.

The structural recovery rate can be modeled by taking into account the nonexponentiality of the structural recovery process [40–42]. The recovery rate depends nonlinearly on temperature and has been accurately determined experimentally for PS [43,44]. Fig. 10a depicts the extracted relaxation enthalpy $\Delta H(\tau_a)$ of isothermally aged PS and nanocomposites as a function of ageing time. For simplicity, we fit our data with a semi-empirical function by Cowie and Ferguson [42]: $\Delta H(\tau_a) = \Delta H_\infty[1 - exp(\tau_a/t_c)^\beta]$, where ΔH_∞ is the asymptotic value for ΔH after an infinite ageing time (τ_a) while t_c is the average relaxation time and β is related to the width of the distribution of relaxation times.

Fig. 10a quantifies the decrease in relaxation enthalpy *at constant temperature* in the presence of fullerenes. This 'apparent' ageing suppression can be attributed to either a trivial difference in ΔT, since T_g of nanocomposites increases with C_{60} due to attractive polymer-filler interfacial interactions, or to a polymer confinement effect induced by the nanoparticle network. To test this hypothesis, we compare the ageing of the PS and nanocomposites at the same

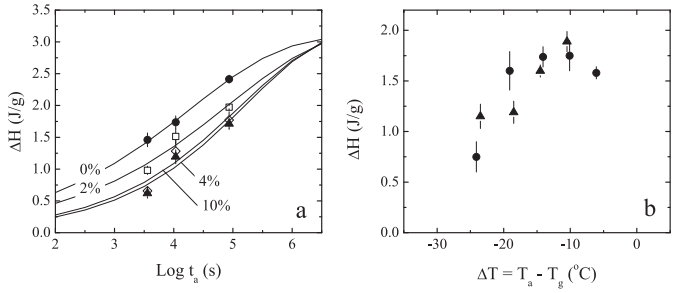

Fig. 10. (a) Relaxation enthalpy ΔH for (•) neat PS270k and composites with (□) 2%, (▲) 4% and (◆) 10% C_{60}, isothermally aged at 90 °C as a function of ageing time. Lines are fits based on the Cowie and Ferguson relaxation model [42] (b) Dependence of the relaxation enthalpy with ageing temperature T_a for (•) neat PS and (▲) PS-C_{60} 4% (τ_a = 180 min), rescaled by their respective T_g.

ΔT ($T_a - T_g$). Fig. 10b shows the dependence of ΔH with T_a at constant ageing time τ_a = 180 min for PS and PS-C_{60} 4%. These results show that both curves largely superimpose after rescaling the ageing temperatures by their respective T_g. The changes in physical ageing at a given τ_a, due to the presence of the fullerenes appear to be, at least in part, attributable to their respective T_g changes (see Fig. 4a). These results suggest that the ageing 'suppression' largely reflects the T_g increase caused by the incorporation of C_{60}. A detailed study separating the asymptotic ΔH_∞ and ageing rates, over longer experimental times, is necessary to accurately elucidate the process and this task is currently underway.

Physical ageing of polymer-nanocomposites, confined polymers, and thin films, exhibiting T_g shifts of various signs, remains controversial [45] in part due to the complex interpretation of structural relaxation. Physical ageing of nanocomposites involving sub 100-nm nanoparticle with attractive polymer-filler interactions, and thus increased T_g (e.g. PMMA/silica and P2VP-silica [4,46]), have been found to exhibit reduced or suppressed physical ageing. Our combined DS and DSC study indicates that PS-C_{60} falls in this trend of nanocomposites with attractive interactions, increased T_g and slower segmental relaxation, and thus suppressed physical ageing. As discussed above, our results can be rationalized, within measurement uncertainty, by the T_g shift imparted by the presence of the fillers.

3.4. Fullerenes and molecular packing

We have previously shown by inelastic incoherent neutron scattering that C_{60} fullerenes increase, albeit modestly, the mean-square proton displacement (*msd*), as measured by the Debye-Waller factor, of glassy polystyrene [14]. At the same temperature, the *msd* of PS increases in the presence of C_{60}, corresponding to a larger amplitude of atomic scale motion (of the order of ≃Å, and high frequency, 10^{-15} s^{-1}), interpreted as a softening of the local vibrational potential in the glassy state. The high frequency softening, for modest C_{60} concentrations (0.7–4) mass %, evidently occurs simultaneously with a slowing down of segmental relaxation leading to an increase of the T_g. This process, as measured by dielectric spectroscopy over typical frequencies of 10^{-2}–10^6 s^{-1}, probes lengthscales of 2–3 repeat units and 100 s timescale at T_g. Fullerenes thus impact PS dynamics in a non-trivial manner. Indeed, this effect is *exactly* opposite to antiplasticizer additives that are characterized by enhancing stiffness in the glassy state, while simultaneously decreasing the T_g [47,48]. By contrast, common 'plasticizers' speed up both the fast dynamics and rate of the α structural relaxation.

Recent simulations [49] suggest that antiplasticization can be understood as arising from an enhancement of molecular packing (reduction of packing frustration) and corresponding reduction in the fragility of glass-formation (a measure of how much the relaxation deviates from an Arrhenius temperature dependence, systems exhibiting a stronger deviation being more 'fragile' in the usual jargon). A disruption of molecular packing at a nanoscale can then be expected to enhance fragility and packing frustration and an increase in T_g can naturally be expected in some systems where this effect is large. Indeed, we find that fullerene in PS appear to be 'fragility enhancing' [50] and can thus be expected to also enhance gas permeability in the glass state, an effect observed with other nanoparticles [2] (and opposite to antiplasticizers that enhance the efficiency of molecular packing), and possibly also ductility, extension at break and other properties correlated with relatively high 'free volume'.

Simulations of the effect of nanoparticles with different interactions on the dynamic fragility m of glass forming polymers [48], relate such increases of fragility to attractive

polymer–nanoparticle interactions that increase the cooperativity of atomic motion in the polymer melt. The strong pi–pi interactions between the fullerene and the aromatic groups of the polystyrene probably account for this attractive interaction. The attractive interaction should thus lead to a local stiffening of the polymer matrix about the nanoparticle (which should in turn affects the nanoparticle dynamics more globally). Presumably from the discussion above, the polymer segments near the nanoparticle exhibit a higher packing efficiency near the particle, but the segments further from the particle are in a more frustrated packing state. It is emphasized that the variations in the local density accessible in these simulations is rather subtle so that it has not yet been possible to directly confirm the packing frustration explanation of the observed fragility changes for nanoparticles exhibiting an attractive polymer–nanoparticle interaction [48].

Fullerenes (and antiplasticizers) evidently have a non-trivial influence on molecular packing and the nature of glass-formation, demonstrating that considerable control can be exerted on the properties of glassy materials through the judicious choice of additive. Clearly, the term plasticizer or antiplasticizer does not capture the complexity of the phenomenon since the high frequency dynamics can change with the additive in a different way from the low frequency α-relaxation dynamics associated with the glass-transition itself. Indeed, recent experimental studies [51,47] have shown that additives can act as both plasticizers below T_g and antiplasticizers above T_g, or vice versa.

3.5. Comparative observations for PS nanocomposites

Nanoparticles have the ability to both increase or decrease T_g of polymers and in Fig. 11 we compile observations on various polystyrene-nanoparticle composites where T_g shifts of both signs are apparent. These trends in T_g do not capture the whole story, since these can be largely independent of changes in the high frequency dynamics, as our discussion in the previous section demonstrates. Unfortunately, limited data considers the high and low frequency dynamics for the same nanocomposite making it hard to conclude much more than a common trend in T_g shifts with polymer–nanofiller interaction.

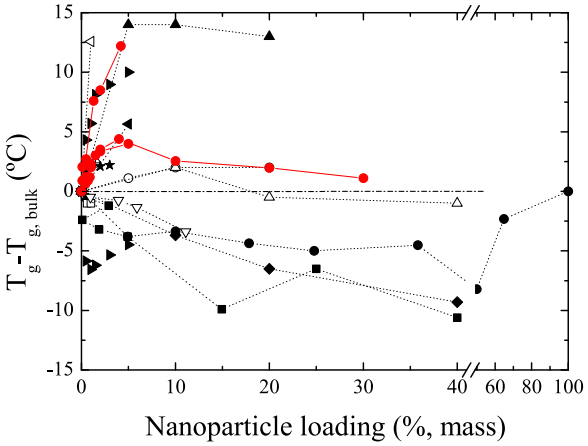

Fig. 11. Glass transition temperature shift of PS upon addition of nanofillers: (▷) PS-grafted gold nanoparticles [52], (•) crosslinked PS nanoparticles [53], (▽) surface modified CdSe [54], (■)SiO_2 [6], (□) SiO_2 [4], (◁) MMT clay [55], (★) SWNT [56], (⊕) 4-(10-hydroxydecyl) benzoate-SWNT [56],⊠ solvent cast C_{60} [57], (▲) solvent cast C_{60} [34], (○) directly mixed C_{60} [34], (△) butylated C_{60} [34], (◆) dodecylated C_{60} [34], (•) [red] rapid precipitation C_{60} of 2-270k PS (present work). (For interpretation of the references to color in this figure legend, the reader is referred to the web version of this article.)

These observations lead us to ask what physical characteristics of an additive are able to tune the 'nature' of glass-formation. Previous work on antiplasticizers suggest that such additives must be smaller than the polymer statistical segment size and should have a strong cohesive interaction with the polymer to inhibit phase separation [58]. What then makes a nanoparticle additive exhibit the contrary effects seen in the present PS-C_{60} measurements?

It is known from studies of thin polymer films [13,11] that the cohesive interaction between the polymer and the substrate can influence the sign of the shift of T_g and the corresponding interaction between the particle and the polymer matrix can be expected to give rise to a similar effect. Polymer nanocomposites are similarly characterized by large interfacial areas and polymer–particle interactions can be somewhat tuned by surface grafting (cf. Fig. 11). For example, Weng et al. [34] demonstrated that substituted and unsubstituted C_{60} could induce, respectively, positive and negative T_g shifts in PS. Overall, the observations confirm the expectation that stronger cohesive interaction tends to give larger upwards shifts of T_g [34,56,55,19,59,4,8], but negative shifts are also observed [54,6,60,8] when the interactions are presumably less favorable, as in crosslinked PS particles and CdSe nanoparticles. This behavior is generally observed in simulations [9] where the particles are comparable in size to the R_g of the polymer, i.e., larger than the statistical segment size (~ 1 nm) in amorphous polymers. Particle dispersion has also an evident impact on T_g (and miscibility), as indicated by the varying magnitude (and even sign) of shifts depending on sample preparation and processing method for PS-C_{60} [7,34]. Upon phase separation, large aggregates are expected to act like macroscopic fillers in which little change in the nature of glass-formation arises, as seen in our high fullerene concentration and aggregated measurements.

Particle shape must also be important in these additive induced changes in molecular packing, and highly extended and irregularly shaped attractive particles should be much more effective at disrupting molecular packing and in shifting the T_g upwards through an enhancement of packing frustration. This might rationalize the large upwards shift of T_g seen in the low concentration clay solutions and in the presence of C_{60} clusters up to below the dispersibility threshold. Apart from the many experimental uncertainties in the surface properties of nanoparticles, and the common geometrical polydispersity in size and shape, the general tendency of nanoparticles to cluster, impurity effects and diverse non-equilibrium effects, the prediction of shifts in T_g is made difficult by subtle changes in both cohesive interactions and molecular packing that can be induced by the nanoparticles. This problem thus requires many further studies to elucidate fully the impact of nanofillers in glass formation, beyond some trends and expectations noted above.

4. Conclusions

We have shown that the addition of C_{60} to PS leads to subtle effects in glass formation, beyond simply changing the glass transition temperature. For dispersed nanocomposites, we find that the glass-transition temperature T_g as well as the dynamic fragility m increases with C_{60} content. The relationship between T_g and m for PS appears to be retained, implying that C_{60} addition has an analogous effect to increasing PS M_W. The physical ageing of these nanocomposites is found to be suppressed, an effect that can be rationalized by the increase in T_g. By contrast, our former incoherent neutron scattering measurements indicate that the local atomic scale 'stiffness' of the material slightly decreases in the glassy state.

So-called 'antiplasticizers' also exhibit opposite dynamic trends of the fast and slow dynamics, and have been associated to relief of packing frustration [49] which, in turn, decreases the fragility of glass formation, effectively changing the nature of glass-formation [48]. Fullerenes in PS appear to induce the exact opposite effect, 'fragilifying' the polymer, also seen for instance with the addition of Aroclor to polycarbonate [47].

The common term 'plasticizer' or antiplasticizer is evidently fraught with difficulties when applied to glass-forming nanocomposites. Not only can the high frequency and α-relaxation processes shift in contrary directions with the additive, but the effect on the high frequency dynamics is often highly temperature dependent. Antiplasticizing additives in the glassy state are often most effective at enhancing (i.e., speeding up) the dynamics at elevated temperatures [58] and around a 'compensation temperature' this behavior changes qualitatively. Evidently, the temperature range of the measurement, along with nature and timescale of the relaxation process, must be specified to apply the terms meaningfully. Indeed a good 'plasticizer' such as water for many polar polymers characteristically leads to sluggish ageing in glassy commercial materials such as epoxies and biological materials such as seeds exposed to moisture [61].

A capacity to tune the high frequency dynamics of glassy materials with additives may also benefit the understanding of the long-term evolution of glassy materials, including non-linear deformation properties, since the high frequency dynamics is the only really active motion in the glassy state. Evidently, nanoparticle additives have the potential to alter the glassy nature of polymers with profound practical ramifications for the control of this ubiquitous class of materials.

Acknowledgments

We acknowledge the Royal Society (UK) and EPSRC (EP/D058414/1) for financial support and the Spanish Ministry of Science (Ministerio de Educación y Ciencia) for a postdoctoral fellowship (AS), and the British Council and the British High Commission Singapore for a Collaborative Development Award 2014–2015. We are grateful to ISIS neutron pulsed source for beamtime and experimental support.

References

[1] Bockstaller M, Mickiewicz R, Thomas E. Block copolymer nanocomposites: perspectives for tailored functional materials. Adv Mater 2005;17(11):1331–49.
[2] Merkel TC, Freeman BD, Spontak RJ, He Z, Pinnau I, Meakin P, et al. Ultrapermeable, reverse-selective nanocomposite membranes. Science 2002;296:519–22.
[3] Krishnamoorti R, Vaia RA. Polymer nanocomposites. J Polym Sci Part B Polym Phys 2007;45(24):3252–6.
[4] Rittigstein R, Priestley R, Broadbelt L, Torkelson J. Model polymer nanocomposites provide an understanding of confinement effects in real nanocomposites. Nat Mater 2007;6:278–82.
[5] Kropka J, Putz K, Pyramitsyn V, Ganesan V, PF G. Origin of dynamical properties in PMMA-C_{60} nanocomposites. Macromolecules 2007;40:5424–32.
[6] Bansal A, Yang H, Li C, Cho K, Benicewicz B, Kumar SK, et al. Quantitative equivalence between polymer nanocomposites and thin polymer films. Nat Mater 2005;4:693–8.
[7] Mackay ME, Tuteja A, Duxbury PM, Hawker B, J C, Van Horn Z, et al. General strategies for nanoparticle dispersion. Science 2006;311:1740–3.
[8] Oh H, Green PF. Polymer chain dynamics and glass transition in athermal polymer/nanoparticle mixtures. Nat Mater 2009;8:139–43.
[9] Starr FW, Schroder TB, Glotzer SC. Effects of a nanoscopic filler on the structure and dynamics of a simulated polymer melt and the relationship to ultrathin films. Phys Rev E 2001;64:21802.
[10] Keddie JL, Jones RAL, Cory RA. Size-dependent depression of the glass transition temperature in polymer films. Europhys Lett 1994;27:59–64.
[11] Forrest JA, Dalnoki-Veress K. The glass transition in thin polymer films. Adv Coll Interf Sci 2001;94:167–264.
[12] Ellison CJ, Ruszkowski RL, Fredin NJ, Torkelson JM. Dramatic reduction of the effect of nanoconfinement on the glass transition of polymer films via addition of small-molecule diluent. Phys Rev Lett 2004;92:095702.
[13] Alcoutlabi M, McKenna GB. Effects of confinement on material behaviour at the nanometre size scale. J Phys Condens Matter 2005;17:R461–524.
[14] Sanz A, Ruppel M, Douglas JF, Cabral JT. Plasticization effect of C_{60} on the fast dynamics of polystyrene and related polymers: an incoherent neutron scattering study. J Phys Condens Matter 2008;20(10):104209.
[15] Wong HC, Sanz A, Douglas JF, Cabral JT. Glass formation and stability of polystyrene-fullerene nanocomposites. J Mol Liq 2010;153:79–87.
[16] Sariciftci NS, Smilowitz L, Heeger AJ, Wudl F. Photoinduced electron transfer from a conducting polymer to buckminsterfullerene. Science 1992;258:1474.
[17] Wong HC, Li Z, Tan CH, Zhong H, Huang Z, Bronstein H, et al. Morphological stability and performance of polymerfullerene solar cells under thermal stress: the impact of photoinduced $PC_{60}BM$ oligomerization. ACS Nano 2014;8(2):1297–308.
[18] Vogiatzis GG, Theodorou DN. Local segmental dynamics and stresses in polystyrene-C_{60} mixtures. Macromolecules 2014;47(1):387–404.
[19] Kropka JM, Garcia-Sakai V, Green PF. Local polymer dynamics in polymer-C_{60} mixtures. Nano Lett 2008;8:1061–5.
[20] Higgins JS, Benoit HC. Polymers and neutron scattering. Oxford Science Publications; 1996.
[21] Certain equipment, instruments or materials are identified in this paper in order to adequately specify the experimental details. such identification does not imply recommendation by the nist nor does it imply the materials are necessarily the best available for the purpose.
[22] Dattani R, Michels R, Nedoma AJ, Schweins R, Westacott P, Huber K, et al. Conformation and interactions of polystyrene and fullerenes in dilute to semidilute solutions. Macromolecules 2014;47(17):6113–20.
[23] Dattani R, Cabral JT. Polymer fullerene solution phase behaviour and film formation pathways. Soft Matter 2015;11:3125–31.
[24] Hutchinson J. Physical ageing of polymers. Prog Polym Sci 1995;20:703–60.
[25] Strobl G. The physics of polymers: concept for understanding their structures and behavior. Germany: Springer; 1996.
[26] Wong HC, Cabral JT. Mechanism and kinetics of fullerene association in polystyrene thin film mixtures. Macromolecules 2011;44(11):4530–7.
[27] Wong HC, Cabral JT. Spinodal clustering in thin films of nanoparticle-polymer mixtures. Phys Rev Lett 2010;105:038301.
[28] Waller JH, Bucknall DG, Register RA, Beckham HW, Leisen J, Campbell K. C_{60} fullerene inclusions in low-molecular-weight polystyrene - poly(-dimethylsiloxane) diblock copolymers. Polymer 2009;50:4199–204.
[29] Jin Y, Cheng JL, Varma-Nair M, Liang G, Fu Y, Wunderlich B, et al. Thermodynamic characterization of C_{60} by differential scanning calorimetry. J Phys Chem 1992;96:5151–6.
[30] Diky VV, Zhura LS, Kabo AG, Markov VY, G. J K. High-temperature heat capacity of C_{60} fullerene. Fullerenes Nanotub Carbon Nanostructures 2001;9:543–51.
[31] Heiney PA, Fischer JE, McGhie AR, Romanow WJ, Denenstein AM, McCauley Jr JP, et al. Orientational ordering transition in solid C_{60}. Phys Rev Lett 1991;66:2911–4.
[32] Rahedi AJ, Douglas JF, Starr FW. Model for reversible nanoparticle assembly in a polymer matrix. J Chem Phys 2008;128:024902–9.
[33] Starr FW, Douglas JF, Glotzer SC. Origin of particle clustering in a simulated polymer nanocomposite and its impact on rheology. J Chem Phys 2003;119:1777–88.
[34] Weng D, Lee HK, Levon K, Mao J, Scrivens WA, E. B S, et al. The influence of buckminsterfullerenes and their derivatives on polymer properties. Eur Polym J 1999;35:867–78.
[35] Mu M, Seitz ME, Clarke N, Composto RJ, Winey KI. Polymer tracer diffusion exhibits a minimum in nanocomposites containing spherical nanoparticles. Macromolecules 2011;44(2):191–3.
[36] Sokolov AP, Novikov VN, Ding Y. Why many polymers are so fragile. J Phys Condens Matter 2007;19(20):205116.
[37] Santangelo PG, Roland CM. Molecular weight dependence of fragility in polystyrene. Macromolecules 1998;31:4581–5.
[38] Kunal K, Robertson CG, Pawlus S, Hahn SF, Sokolov AP. Role of chemical structure in fragility of polymers: a qualitative picture. Macromolecules 2008;41(19):7232–8.
[39] Pazmino Betancourt BA, Douglas JF, Starr FW. Fragility and cooperative motion in a glass-forming polymer-nanoparticle composite. Soft Matter 2013;9:241–54.
[40] Moynihan CT, Macedo PB, Montrose CJ, Gupta PK, DeBolt MA, Dill PF, et al. NY Acad Sci 1976;15:279.
[41] Kovacs AJ, Aklonis JJ, Hutchison JM, Ramos AR. J Polym Sci Polym Phys 1979;17:1097.
[42] Cowie JMG, Ferguson R, McEwen IJ. Physical aging studies in poly(viny1 methyl ether). 1. enthalpy relaxation as a function of aging temperature. Macromolecules 1989;22:2307–12.
[43] Simon SL, Sobieski JW, Plazek DJ. Volume and enthalpy recovery of polystyrene. Polymer 2001;42:2555–67.
[44] Brunacci A, Cowie JMG, Ferguson R, McEwen IJ. Enthalpy relaxation in glassy polystyrenes: 1. Polymer 1997;38:865–70.
[45] Cangialosi D, Boucher VM, Alegria A, Colmenero J. Physical aging in polymers and polymer nanocomposites: recent results and open questions. Soft Matter 2013;9:8619–30.

[46] Rittigstein P, Torkelson JM. Polymer-nanoparticle interfacial interactions in polymer nanocomposites: confinement effects on glass transition temperature and suppression of physical aging. J Polym Sci Part B Polym Phys 2006;44:2935–43.
[47] Psurek T, Soles CL, Page KA, Cicerone MT, Douglas JF. Quantifying changes in the high-frequency dynamics of mixtures by dielectric spectroscopy. J Phys Chem B 2008;112:15980–90.
[48] Starr FW, Douglas JF. Modifying fragility and collective motion in polymer melts with nanoparticles. Phys Rev Lett 2011;106:115702.
[49] Riggleman RA, Yoshimoto K, Douglas JF, de Pablo JJ. Influence of confinement on the fragility of antiplasticized andpure polymer films. Phys Rev Lett 2006;97:045502.
[50] 'Fragility' is quantified by the deviation from an Arrhenius temperature dependence of structural relaxation, which is normally taken as an ideal fluid behavior. Increasing 'packing efficiency' of fluids leads to the formation of 'stronger' glasses. Phenomenologically, fragility is correlated to the breath of glass formation process, rather than to T_g itself. Indeed, fragile liquids exhibit glass transitions over narrower temperature ranges, so that ratios of the characteristic temperatures of glass-formation provide a convenient measure of fragility.
[51] Miyazaki T, Nishida K, Kanaya T. Contraction and reexpansion of polymer thin films. Phys Rev E 2004;69:022801.
[52] Chen F, Clough A, Reinhard BM, Grinstaff MW, Jiang N, Koga T, et al. Glass transition temperature of polymernanoparticle composites: effect of polymerparticle interfacial energy. Macromolecules 2013;46(11):4663–9.
[53] Mackay ME, Dao TT, Tuteja A, Ho DL, Van Horn B, Kim HC, et al. Nanoscale effects leading to non-Einstein-like decrease in viscosity. Nat Mater 2003;2:762–6.
[54] Lee JY, Su KE, Chan EP, Zhang Q, Emrick T, Crosby AJ. Impact of surface-modified nanoparticles on glass transition temperature and elastic modulus of polymer thin films. Macromolecules 2007;40:7755–7.
[55] Chen K, Wilkie CA, Vyazovkin S. Nanoconfinement revealed in degradation and relaxation studies of two structurally different polystyreneclay systems. J Phys Chem B 2007;111(44):12685–92.
[56] Pham JQ, Green PF. Effective tg of confined polymer-polymer mixtures. influence of molecular size. Macromolecules 2003;36:1665–9.
[57] Bershtein VA, Egorov VM, Zgonnik VN, Melenevskaya EY, Vinogradova LV. Anomalises of glass transition: manifestation in fullerene core polystyrene stars. J Therm Analysis Calorim 2000;59:23–31.
[58] A. Anopchenko, T. Psurek, D. VanderHart, J. F. Douglas, J. Obrzut, Dielectric study of the antiplasticization of trehalose by glycerol, Phys Rev E 74.
[59] Kotsilkova R, Fragiadakis D, Pissis P. Reinforcement effect of carbon nanofillers in an epoxy resin system: rheology, molecular dynamics, and mechanical studies. J Polym Sci Part B Polym Phys 2005;43:522–33.
[60] Ash BJ, Siegel RW, Schadler LS. Glass-transition temperature behavior of alumina/PMMA nanocomposites. J Polym Sci Part B Polym Phys 2004;42:4371–83.
[61] Zheng Y, McKenna GB. Structural recovery in a model epoxy: comparison of responses after temperature and relative humidity jumps. Macromolecules 2003;36(7):2387–96.